MONTANA
TECHNOLOGICAL UNIVERSITY

June 14, 2021
Mr. John M. Fitzgerald, ESQ
Fitzgerald Law Firm
343 Quincy Street; Ste 101
Rapid City, SD 57701

Re: **Geophysical investigations to determine the unknown extents of the abandoned Blackhawk gypsum mine, Blackhawk, SD**

Dear Mr. Fitzgerald:

As requested, we have performed a geophysical survey for the referenced project. The purpose of this evaluation was to determine the extent of the abandoned gypsum mine, i.e., to explore the possibility of the existence of mine working areas (voids) beyond the known extent of the abandoned mine, in the Hideaway Hills Subdivision, Blackhawk, SD.

The fieldwork, analyses, and findings of this report were conducted following generally accepted geophysical practices.

Please do not hesitate to contact me for any additional information.

Respectfully submitted,

Mohammadhossein Sadeghiamirshahidi, Ph.D., A.M.ASCE.
Assistant Professor
Geological Engineering Department
Montana Technological University
1300 West Park Street
Butte, MT 59701

Attached: BlackHawk Geophysical Investigation report

MONTANA
TECHNOLOGICAL UNIVERSITY
1300 West Park Street | Butte, MT 59701 | 800.445.8324

6/10/2021

Geophysical investigations to determine the unknown extents of the abandoned Blackhawk gypsum mine, Blackhawk, SD

Prepared by:

Mohammadhossein Sadeghiamirshahidi
Ph.D., A.M. ASCE.

Assistant Professor
Geological Engineering Department
Montana Technological University
1300 West Park Street
Butte, MT 59701

Mohamed Khalil
Ph.D.

Former Assistant Professor
Geophysical Engineering Department
Montana Technological University
1300 West Park Street
Butte, MT 59701

Prepared for:

Fitzgerald Law Firm
343 Quincy Street; Ste 101
Rapid City, SD 57701

TABLE OF CONTENTS

LIST OF TABLES

LIST OF FIGURES

INTRODUCTION

On April 27th, 2020, a sudden ground collapse (sinkhole) appeared in the Hideaway Hills Subdivision, Blackhawk, South Dakota (Figure 1). After a group of cavers from Paha Sapa Grotto (an internal organization of the National Speleological Society located in the Black Hills of South Dakota) investigated the sinkhole, it was determined that the sinkhole was related to a shallow abandoned gypsum mine. About half a dozen families were forced to evacuate the premises while many others have voluntarily evacuated their houses out of fear. It is worth mentioning that, apart from this recent sinkhole, there are other possible indicators of subsidence throughout the subdivision, e.g., growing cracks on the roads and sidewalks.

Figure 1. April 27th, 2020 Sinkhole, Hideaway Hills Subdivision, Blackhawk, SD. (picture was taken in May 2021)

In order to develop a hazard map for the area that can be used for issuing proper evacuation notices, the exact extent of the abandoned mine needs to be known. There is limited information available about this mine, from which the exact extent of the mine can not be determined with a desired degree of certainty. Although an approximate map of the underground mine was produced by the cavers (see Figure 2), the exact extent of the mine could not be determined due to some obstacles. The eastern part of the underground mine was flooded (filled with water) which made it impossible to access and map the mine beyond that point. Also, what appeared to

be collapsed zones according to the cavers, restricted access to the northern, southern, and western boundaries of the underground mine.

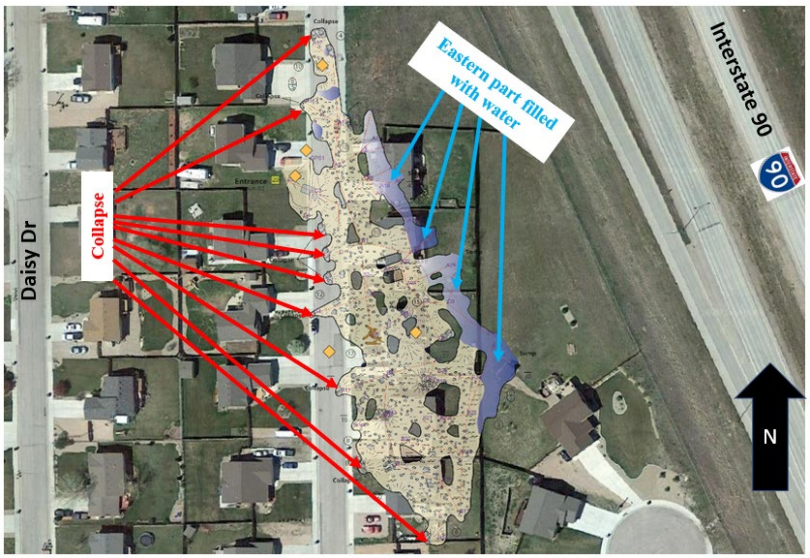

Figure 2. Approximate extent of the underground mine developed by Paha Sapa Grotto cavers (Wolfe et al. 2020) overlaid on the subdivision by Patrick Ealy, Fitzgerald Law Firm (Zionts 2020)

The main purpose of this project was to use non-destructive geophysical methods to examine the possibility of the existence of mine working areas (voids) beyond the known extent of the abandoned mine, i.e., better understand the extent of the abandoned mine.

BACKGROUND SUMMARY

The underground Blackhawk mine was operated by the Dakota Plaster company starting from 1912. The first report on the Blackhawk Mine, that the authors could find, was from the South Dakota state mine inspector in 1912 (Aberdeen 1928). There is not enough data from the first year but it seems that the mine only produced gypsum part of the first year. Also, from 1919 to 1921, the underground mine did not produce gypsum, as the Dakota Plaster Company was taking gypsum from the surface. It is, however, unclear if the gypsum was mined from an outcrop of the Spearfish Formation (the gypsum bearing formation), or if it was taken from the gypsum that was already mined from the underground mine and stockpiled on the surface. In 1924, the Dakota Plaster Company secured a contract to supply gypsum for the state cement plant for the next year. No mining information could be found for the underground mine after 1926. It is speculated that the lack of accurate mining history for the area is because, prior to 1983, the state of South Dakota did not require a license to mine gypsum, sand, gravel, and other materials used to produce cement. Table 1 summarizes the annual gypsum production from the Blackhawk mine from 1912-1926 (Aberdeen 1928).

Table 1. Annual gypsum production (Aberdeen 1928)

Year	Tons of Gypsum Produced
1912	No data
1913	10,760
1914	10,000
1915	9,105
1916	4,070 (mill destroyed by fire)
1917	3,915
1918	3,000
1919	3,956 (No underground mining, gypsum was taken from the surface)
1920	1,495 (No underground mining, gypsum was taken from the surface)
1921	3,933 (No underground mining, gypsum was taken from the surface)
1922	2,127+1488
1923	3,327
1924	1,707
1925	5,035
1926	1,877 (last yearly mine inspection found)
1912-1926 total	66,095

Figure 3 shows the approximate locations of the past and present known mining activities in the Blackhawk area. The locations identified by the blue polygons in the figure are reclaimed surface gypsum mines. The location identified by the red polygon 1 is an active surface gypsum mine, and the location identified by the red polygon 2 is an active surface sand and gravel mine.

The approximate location of the underground Blackhawk mine is identified with the yellow polygon.

Figure 3. Approximate location of known mining activities in the area

The Blackhawk underground mine was targeting a gypsum bed in the Spearfish Formation. The Spearfish Formation is a 402 - 497 ft (122 - 151 m) thick rose to red mudstone and siltstone formation containing gypsum beds of up to 20 ft (6 m) thick. The gypsum beds occur near the middle and near the top of the formation. Also, veins of gypsum occur throughout the formation (Lisenbee and Hargrave 2005). Figure 4 shows the gypsum-bearing Spearfish Formation outcrops in the area. As it can be seen, the gypsum-bearing layers are very shallow in the area and even has outcrops in the vicinity to the west of the Blackhawk underground mine.

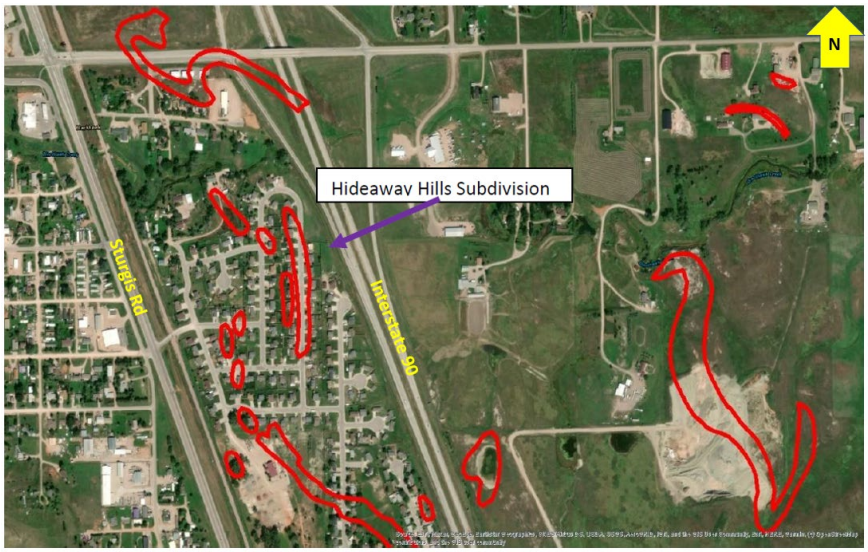

Figure 4. Gypsum bearing Spearfish Formation outcrops in the area

Based on a cross-section presented in the 1:24,000 Geologic map of the Blackhawk quadrangle, South Dakota (Lisenbee and Hargrave 2005), the Spearfish Formation dips towards northeast-east. This implies that the underground mine is unlikely to extend much farther to the west but could extend to a large distance on the north, south, and east side. If the mine does extend on the west side, however, the depth of the mine would be very shallow which allows for more surface disturbance problems such as sinkholes.

Another important parameter in determining the extent of the mine is the location of the groundwater table. Figure 5 shows the contours of the depth to the groundwater table in the area. The contours were developed based on the reported groundwater depths in the well-logs obtained from the South Dakota Department of Environment and Natural Resources.

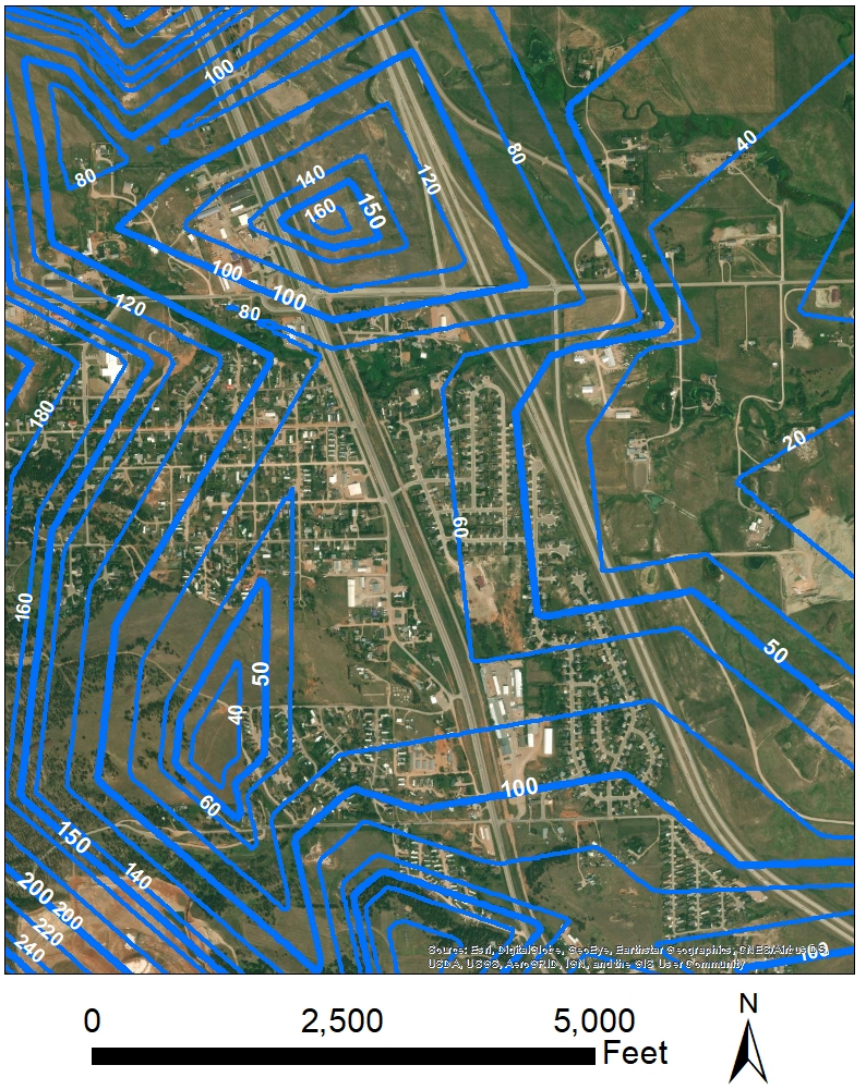

Figure 5. Contours of the depth to the groundwater table (in ft.) in the area

As can be seen from Figure 5, the groundwater table in the abandoned mine area is about 40 to 50 ft deep. According to our estimates based on the information available from the mapped area of the mine (Wolfe et al. 2020), the floor of the mine dips approximately 10.5 degrees in the

N65E direction. The abandoned mine's working areas are 10 to 20 ft deep on the west side of the mapped area and therefore they are above the groundwater table, i.e., not flooded. The abandoned mine's working areas mapped by the cavers on the northeast-east side are, on the other hand, 40-50 ft deep. This is where the mined area starts being flooded and the cavers could not continue the mapping of the mine. According to this information, if the mine extends beyond the mapped area in the northeast-east direction the working areas are expected to be at depths of about 40-50 ft or deeper and they will most likely be flooded.

METHODOLOGY

In this research, a geophysical investigation was conducted in the Hideaway Hills Subdivision, Blackhawk, SD to examine the possibility of the existence of mine working areas (voids) beyond the known extent of the abandoned mine.

In order to map the horizontal distribution of inferred tunnels and cavities, i.e., mined areas, three non-destructive geophysical methods were conducted; (1) Frequency Domain Electromagnetic (FDEM) method, (2) Self-Potential (also known as Spontaneous Potential, SP) method, and (3) Electrical Resistivity Tomography (ERT).

The Frequency Domain Electromagnetic (FDEM) method is a type of electromagnetic or magnetic induction and involves measuring voltages induced in the earth when exposed to a varying frequency domain magnetic field. FDEM is in fact a close source electromagnetic induction method based on Maxwell's laws. FDEM has been used by several researchers (e.g., Soupios et al. 2007) to show the lateral variation of apparent conductivity values and overcome high contact resistance, which enables cross-validation with electrical resistivity measurements.

In Self-Potential (SP) method, naturally occurring electric potential difference in the ground is measured between two electrodes. SP measurements are used as a non-intrusive flow sensor where the electrical potential caused by subsurface current sources such as fluid flow in porous media is measured (Minsley et al. 2011). Streaming potentials are dominated by the electrical double-layer phenomenon as the fluids (groundwater) flow through pore spaces causes an excess drag of the built-up positive charge on mineral grains, expressed as a streaming current density (Revil and Jardani 2010). In SP measurement, the positive self-potentials are attributed to the direction of fluid flow and the negative self-potentials indicate downward seepage. Determining the direction of flow, at least in parts of the study area coinciding with electrical resistivity lines, would help validate the interpretations of the results.

The Electrical Resistivity Tomography (ERT) method utilizes differences and contrasts in electrical resistivity to identify the subsurface geo-material, including voids. In this method, the subsurface bulk electrical resistivity is imaged, which provides information about changes in subsurface lithology and groundwater saturation (Minsley et al. 2011). The resistivity measurements depend on different parameters such as porosity, salinity concentration, clay content especially within unconsolidated sediments, and the existence of voids (Loke 2004). It is worth mentioning that voids could have different signatures when it comes to the bulk electrical resistivity depending on whether they are filled with air, freshwater, or saline water. Their signature is also affected by the size of the void and the surrounding lithology.

Implementation of the FDEM and SP methods

FDEM was measured at more than 525 points in a grid composed of 29 lines in the area. The lines were approximately 10 m apart while the points on each line were 5 m apart. The location of each point was recorded with a handheld GPS and later mapped in google earth pro as shown in Figure 6. The yellow squares in the figure indicate the points where the FDEM measurements were conducted. The conductivity meter EM31, manufactured by Geonics, was used in our investigations. This equipment has an inter-coil spacing of 3.66 m and an operating frequency of 9.8 kHz. The transmitter and receiver coils are used in the horizontal dipole mode (HDM) and the vertical dipole mode (VDM). The depth of investigation is 3 m and 6 m for HDM and VDM,

respectively. The receiver coil measures the ratio of secondary to the primary magnetic field, which is linearly proportional to terrain conductivity, under a low induction number condition (LIN). Both HDM and VDM modes were used at all FDEM points and two apparent resistivity maps at 10ft (~3m) and 20ft (~6m) depths were developed based on the measured data. FDEM maps show the conductivity or resistivity distribution at the two depths as mentioned. It is worth mentioning that FDEM will be affected by any high-power lines in the area.

Figure 6. Locations of the FDEM measurements

To measure self-potential, nonpolarizing electrodes (Lead-Lead Chloride) were used. Each potential measurement was conducted between a variable point and a base station as shown in Figure 7. As the SP measurements change with time, all the measurements were conducted in one day and a drift correction measurement was performed at the end of the day. The same points where the FDEM measurements were taken were used for the SP variable points. However, as it was not possible to measure the SP on the asphalt (or the concrete), only part of the FDEM grid was used to measure the SP as shown in Figure 7. The SP distribution map was developed for the target area to investigate the water flow directions. This would help in the interpretation of the ERT results.

Figure 7. Locations of the base station and variable points used in the SP measurements

Implementation of the ERT methods

For the 2-D resistivity analyses, nine ERT profile lines with different lengths were used in this project as shown in Figure 8. The red stars at the beginning of each line in the figure show the start point of the survey line (X=0 in the resistivity profiles). The survey was completed using a Lippmann resistivity meter (4point light 10W). When conducting ERT surveys, different electrode geometries (arrays) can be used. Each array has its advantages and disadvantages and can yield different resolutions and depths of data. The Wenner and dipole-dipole geometries are the preferred arrays in projects such as this study where shallow features are being investigated (Özel and Darıcı 2020). In the Wenner array, four electrodes of equal spacing, *a,* are used with the current-inducing electrodes (usually known as electrodes A and B) on the outside of the array and potential electrodes (usually known as electrodes M and N) between electrodes A and B (see Figure 9). The Wenner Array has a high vertical resolution, high signal strength, but low data coverage. The Wenner Array reaches an approximate depth of 20% of the distance between current electrodes. In the dipole-dipole array, the current electrodes (A and B) are placed on one side of the array at a distance "a" apart from each other and the potential electrodes are placed on the other side of the array with the same distance "a" between them. The distance between electrodes B and M is always 'n×a' where n is an integer number (see Figure 9). This array is characterized by a low electromagnetic coupling between the current and potential circuits and very sensitive to horizontal changes in resistivity. That means that it is good in mapping vertical structures, such as dykes and cavities. Its maximum depth of investigation is about 21% of the

total length of the array. In this study, different electrode spacings (ranging from 0.5 m to 5 m) were used for different profiles based on the length of each profile. Wenner and dipole-dipole arrays were used for all the profiles. The length and the electrode spacing used for each line are summarized in Table 2.

Figure 8. ERT profile lines used in this project

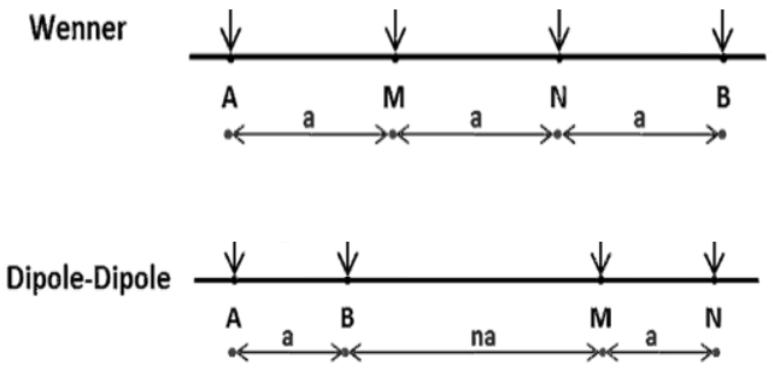

Figure 9. A schematic illustration of the Wenner and Dipole-Dipole arrays used in this study

Table 2. Length and the electrode spacings used in the ERT profile lines

ERT Line	Length (m)	Electrode spacing (m)
Line 1	120	1.5
Line 2	200	2.5
Line 3	320	4
Line 4	40	0.5
Line 5	80	1
Line 6	100	1.25
Line 7	160	2
Line 8	120	1.5
Line 9	200	5

After conducting the ERT survey, 2-D electrical resistivity inversions of the collected data were performed using Res2DINV software. In the inversion process, an initial model of the underground is assumed and the theoretical resistivity for the model is calculated. In an iterative process, the model is continuously adjusted to minimize the difference (error) between the measured and calculated resistivity. The iteration stops and the final model is produced when the lowest possible error is achieved. The inversion algorithm developed by Loke (2004) is based on the finite element technique with a robust constrained least-squares method. The robust inversion, or L1-norm, tends to produce sharp boundaries and more accurately reflect known geology, whereas smoothness constrained or L2-norm reflects smooth variations in the homogenous media such as diffusion boundaries (Loke 2004). Caves and underground mine working areas are expected to produce a sharp anomaly within resistive media. We applied a half-width spacing model refinement, a technique commonly used with large resistivity variations near the ground surface (Loke 1996). The reference model value was the average apparent resistivity value from the given dataset. The model was limited to 10 inversions, although some inversions converged at 4–6 iterations.

It is worth mentioning that determining voids, whether naturally occurring or mined areas, in gypsum strata can be quite challenging (Ulugergerli and Akca 2006; Guinea et al. 2010; Martínez-Moreno et al. 2015, 2018; Moreno 2015; Stafford et al. 2017; Özel and Darıcı 2020).

This is partly because different types of gypsum have different resistivities ranging from 20 ohm-m to more than 1000 ohm-m (Guinea et al. 2010). The voids could also have various resistivity signatures depending on its surrounding lithology and whether it is filled with air, freshwater, saline water, or backfill material/collapsed material. To overcome these challenges, line 4 of the ERT survey was conducted on a gypsum outcrop in the area to have an estimate of the expected resistivity of the gypsum strata. Gypsum rock samples from the outcrop were also taken and compared to the rock samples from the mine to make sure they are from the same source. Lines 6 and 8 were also designed to cover known extends of the mine, both flooded and dry areas, to better understand the expected signature of the voids in the area.

RESULTS AND DISCUSSIONS

In order to identify potential voids beyond the known extent of the abandoned gypsum mine, three non-destructive geophysical methods, i.e., FDEM, SP, and ERT methods, were conducted. The results of each method are presented in this section along with a short discussion of the results.

Frequency domain electromagnetic (FDEM) results

As mentioned before, HDM and VDM modes were used at all FDEM points. Two apparent resistivity distribution maps (one at 3 m depth and one at 6 m depth) were developed based on the measured data as shown in Figure 10. The red dots in the figure are the points where FDEM measurements were taken (see Figure 6). The red arrows in Figure 10 show the approximate location of the smaller sinkhole that opened up around 2016 shown in Figure 11.

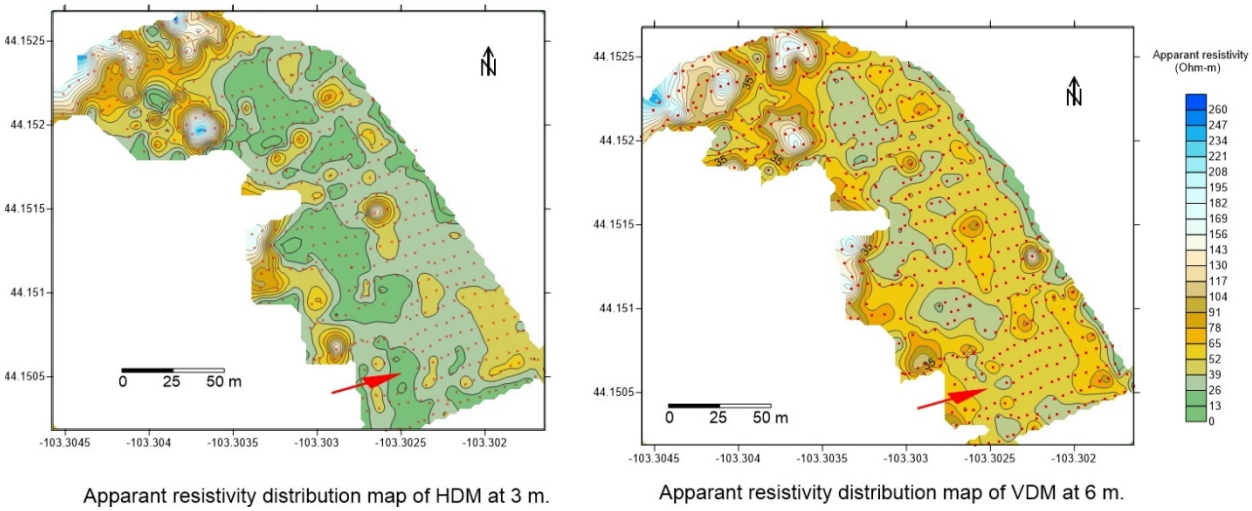

Figure 10. Apparent resistivity distribution maps calculated from FDEM measurements under HDM mode (left figure) and VDM mode (right figure). The red arrows show the approximate location of the 2016 sinkhole.

Figure 11. The smaller sinkhole that occurred around 2016 (picture taken in 2020).

As can be seen in Figure 10, the area around and below this sinkhole appears in both maps as an anomaly. In the apparent resistivity map at 3m depth (left map in Figure 10), the area below this sinkhole appears to have very low resistivity while higher resistivity is shown in the apparent resistivity map at 6m depth (right map in Figure 10). As can be seen in the figure, several other areas with similar patterns can be identified. These areas could be the locations of possible mined areas (voids).

Self-potential (SP) Results

The corrected SP data recorded from the self-potential survey was used to develop a self-potential map that displays the natural potential difference throughout the surveyed area as shown in Figure 12. The negative voltage readings in the SP map indicate a vertical downward flow of water. Therefore, red areas in the SP map indicate the areas of downward flow (seepage) of the saline water which could be another indicator of voids in that area. The green arrow in Figure 12 shows the approximate location of the 2016 sinkhole shown in Figure 11.

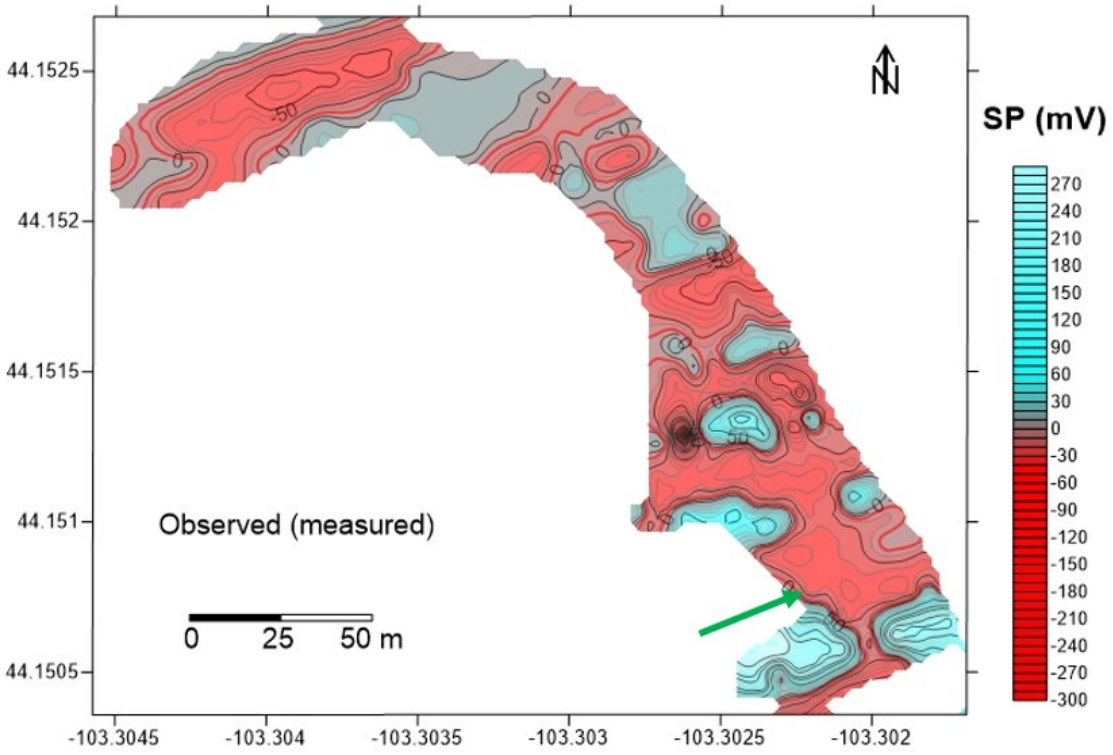

Figure 12. The self-potential (SP) map of the surveyed area

There is a reasonable correlation between the anomalies observed in FDEM maps with downward flow areas observed in the SP map which increases the possibility of the observed anomalies being related to the mined areas (voids).

Electrical resistivity tomography (ERT) results

As mentioned before Wenner and Dipole-Dipole arrays were performed on all nine ERT lines. Both arrays produced similar results so only the results of one array for each line are presented. The ERT models produced for the nine survey lines are presented in Figures 13 to 21.

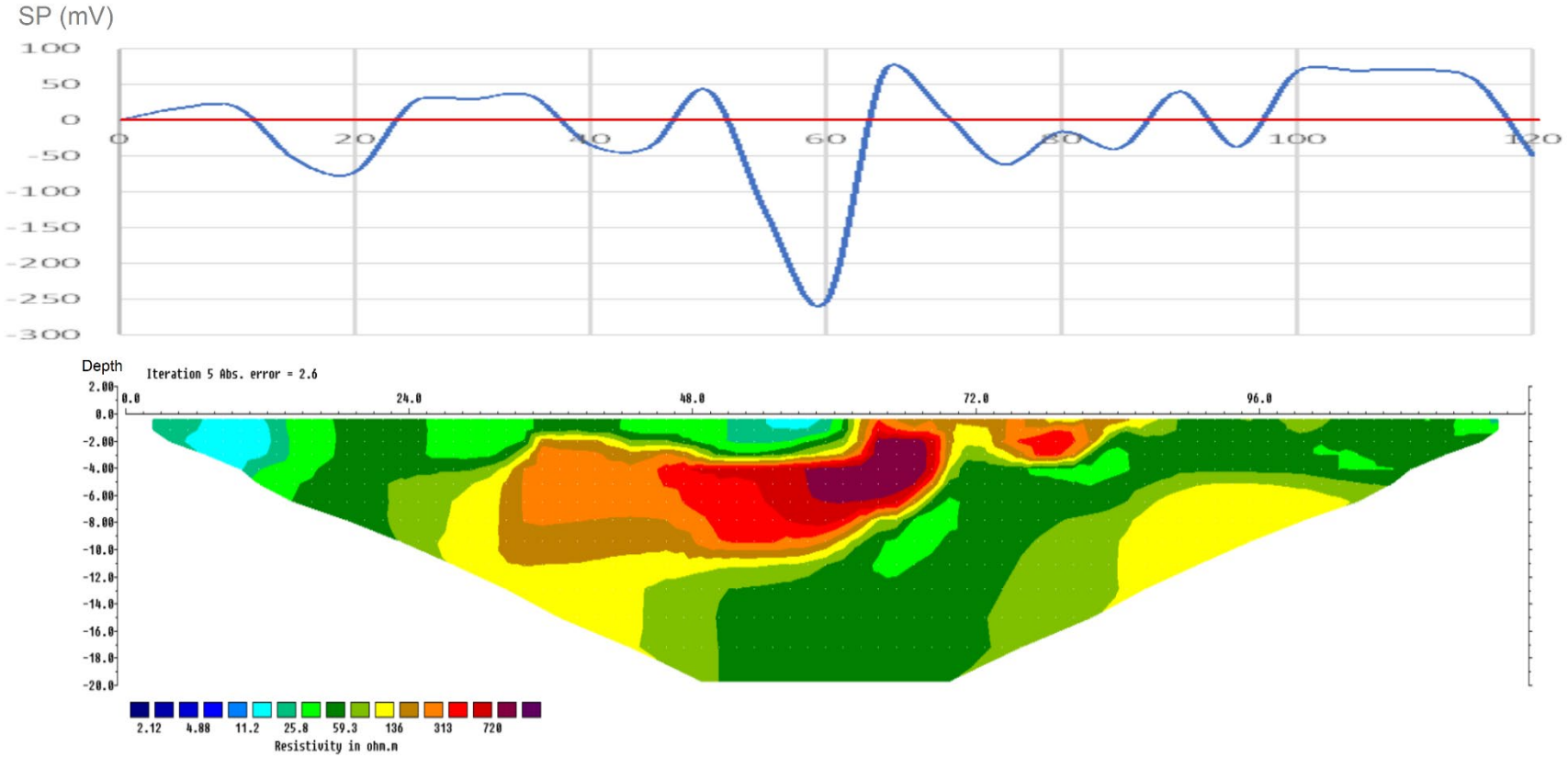

Figure 13. SP (top figure) and ERT model results (bottom figure) for line 1

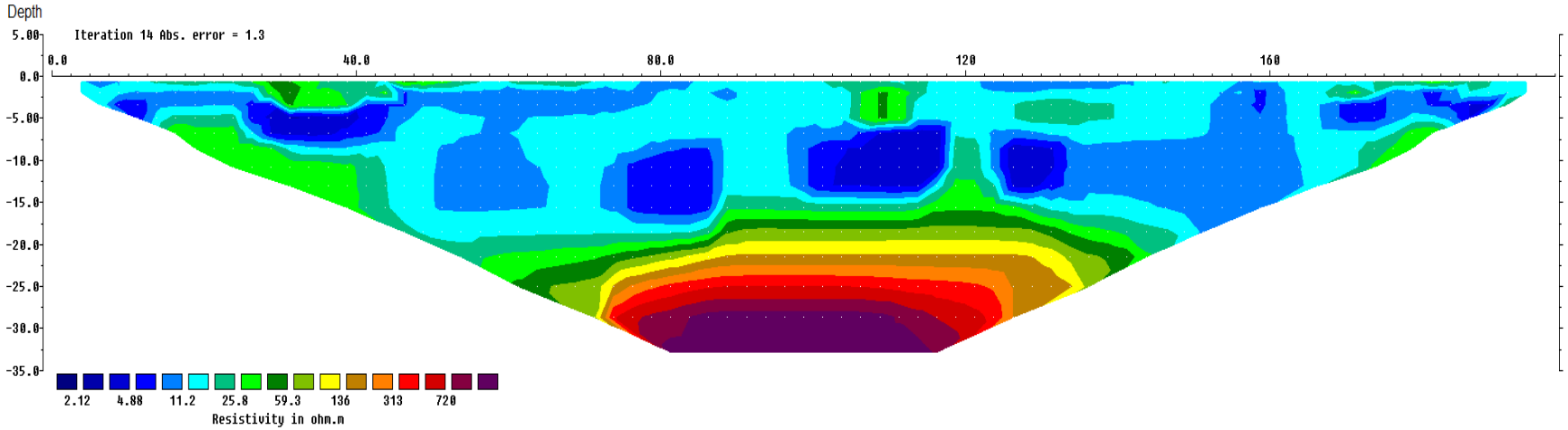

Figure 14. ERT model results for line 2

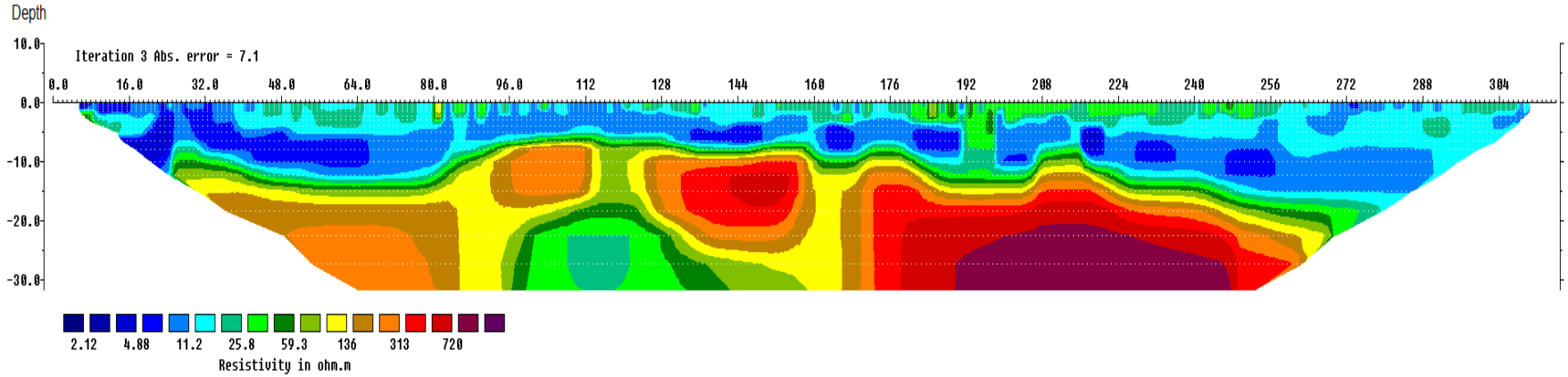

Figure 15. ERT model results for line 3

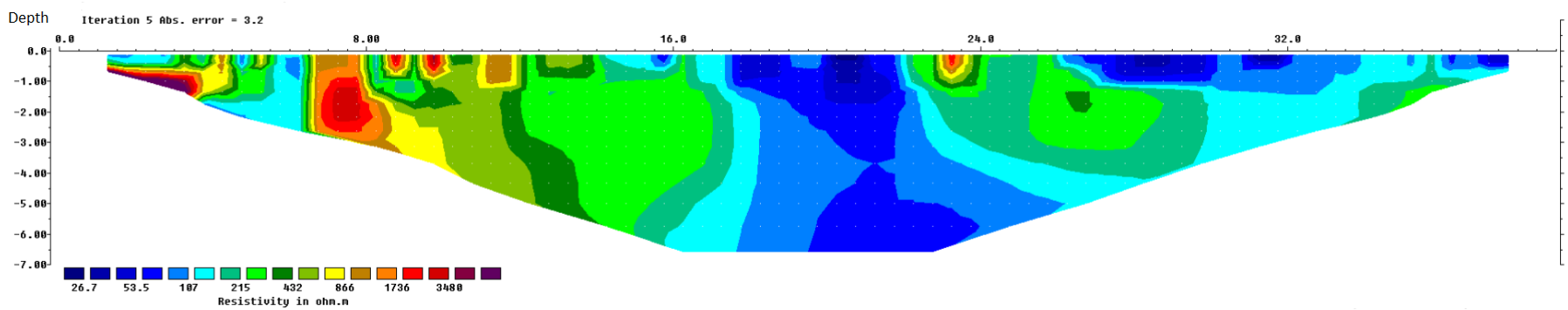

Figure 16. ERT model results for line 4 (gypsum outcrop)

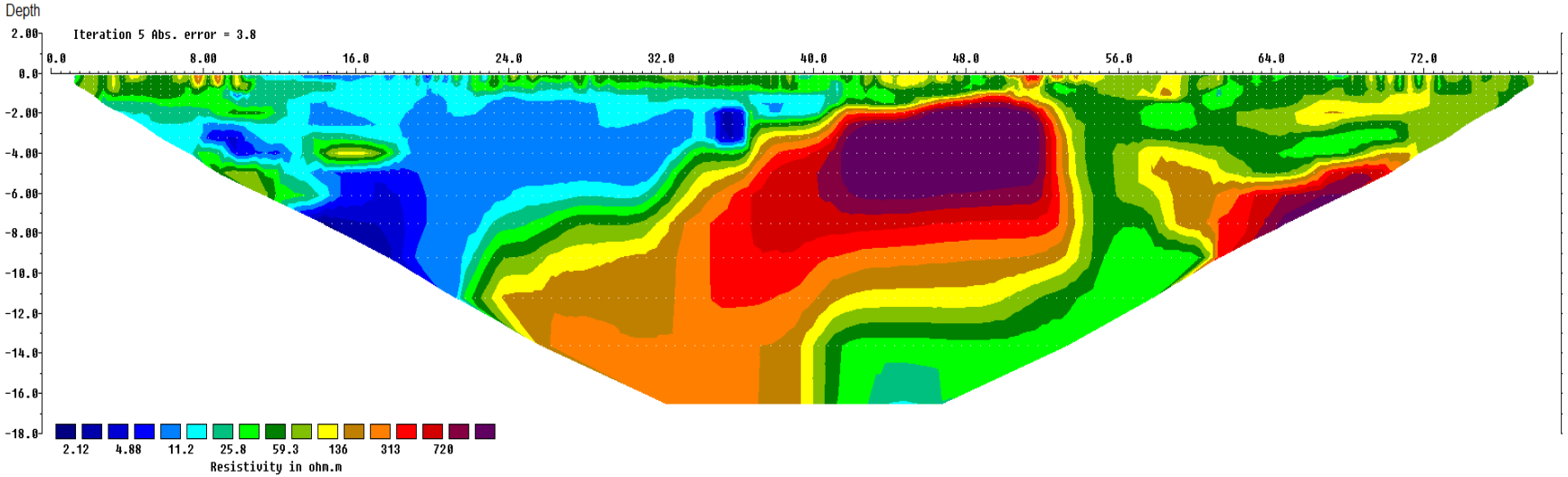

Figure 17. ERT model results for line 5

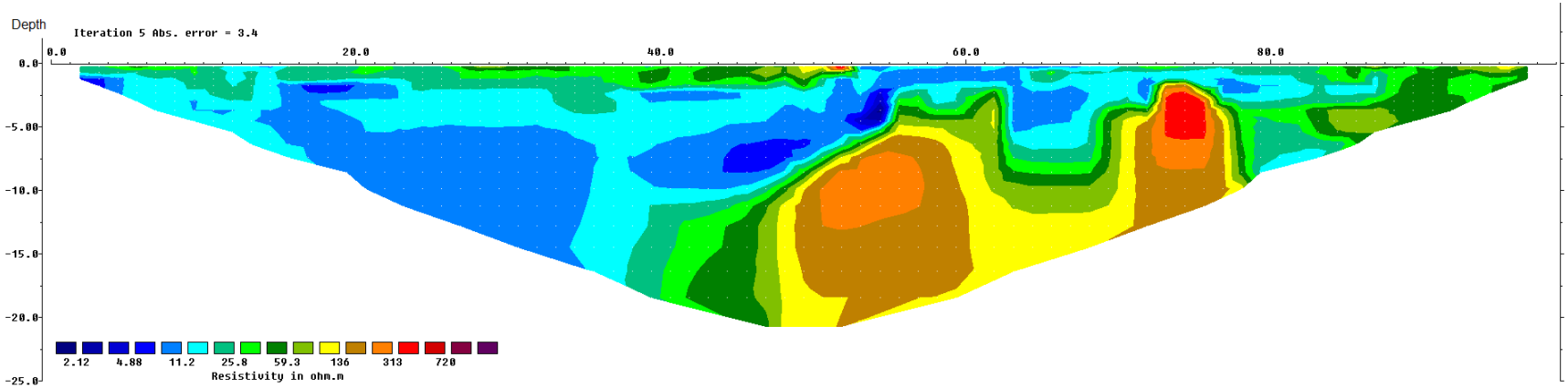

Figure 18. ERT model results for line 6

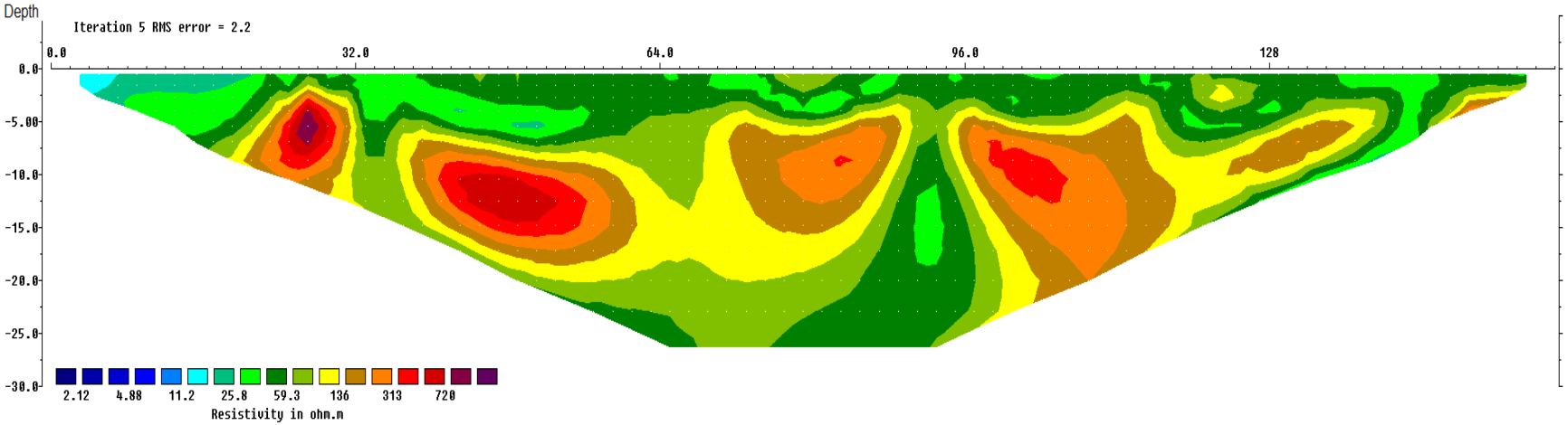

Figure 19. ERT model results for line 7

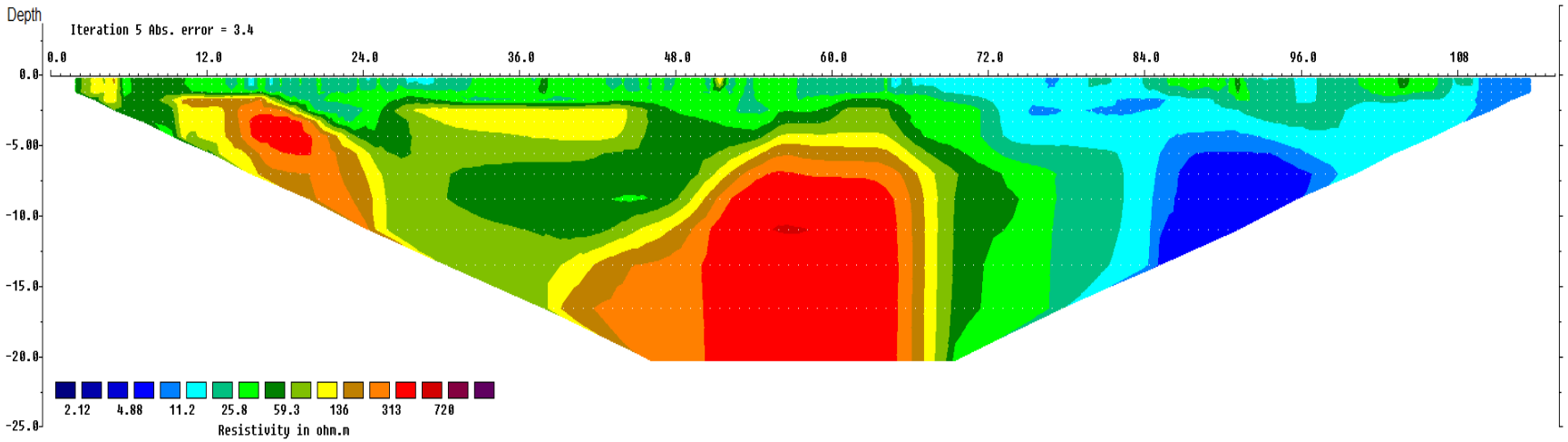

Figure 20. ERT model results for line 8

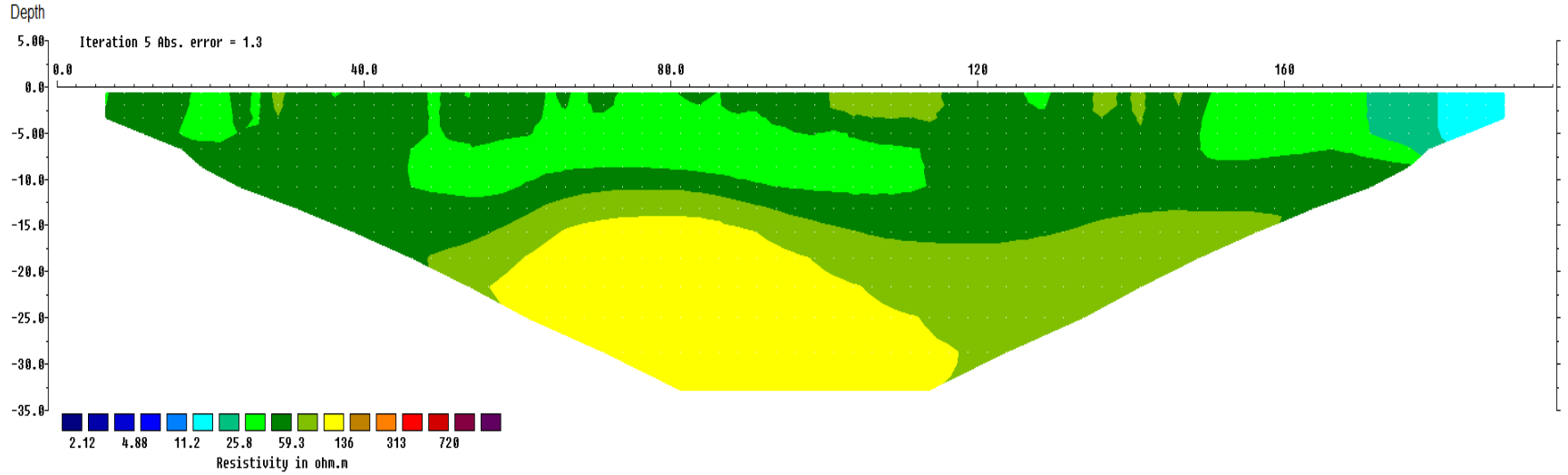

Figure 21. ERT model results for line 9

Figure 16 shows the ERT model for line 4 which was conducted on the gypsum outcrop in the area. The length of this profile was 40 m, and electrode spacing of 0.5 was used to have a high resolution of resistivity data which would help to better understand the resistivity signatures of the gypsum layer. Along line 4, gypsum outcrops were visible from 7 m to 13 m marks (7 m and 13 m from the start point of the profile). From 13 m to 17 m on the profile, a combination of gypsum outcrop and sandy soil intervals were observed (Figure 22).

Figure 22. Gypsum outcrop with sandy soil at about 17 m from the start point of ERT line 4 (sharpie for scale).

From the 5 m to the 6 m marks on line 4, a sandy soil was observed with a texture very similar to beach sand (Figure 23). Samples were taken from this soil and XRD analyses were conducted on the specimens in the Geological Engineering Department of the Montana Technological University. The results showed that this sandy soil is composed of about 50% quartz and about 50% gypsum. This indicates that the soil is probably formed from the disintegration of the outcrop (gypsum with some impurities) and probably some mixing with other soils in the area. Similar sandy soil was also observed about 3 m south of this point next to a disintegrating gypsum rock Figure 24. Similar sand layers were also observed from the 17 m to the 22 m marks, and from the 27 to the 33 m marks on the ERT line 4. Comparing this information with the ERT model of line 4 (Figure 16) indicates that the disintegrated/disintegrating gypsum (sandy layers) is conductive with resistivities in the range of about 25 ohm-m to 160 ohm-m, while the resistivity of the gypsum rock (gypsum seam) itself is in the range of 500 ohm-m to 1000 ohm-m.

Figure 23. A very conductive sand layer at about 6 m from the start point of ERT line 4 (sharpie for scale).

Figure 24. Similar sand layer, seen at about 6 m from the start point of ERT line 4 next to disintegrating gypsum rock

Discussions

ERT-line 1 was conducted on the north-northwest end of the study area (see Figure 8) as the north entrance of the mine is suspected to be located in this area (see Figure 25). ERT-Line 1

was also designed to overlap with one of the lines of the SP grid to help better interpret the results. The SP results for this line are shown in the top part of Figure 13 and the ERT model of line 1 is shown in the bottom part of Figure 13. There is a high resistivity area from 33 m to 69 m marks at a depth of about 1 m to 10 m and another one at 72 m to 84 m marks at 2 m-4 m depth. These areas have resistivities in the range of gypsum resistivity in the study area and could be interpreted as unmined gypsum seams. On the other hand, SP results show high-magnitude negative self-potential values for the same high resistivity areas, especially for the shallow resistivity anomaly (>720 ohm-m) that extends from 61 m to 69 m marks. The negative SP indicates a downward seepage of surface water which could be caused by the existence of voids below the surface. Assuming the north entrance of the mine was in fact at the location that is shown in Figure 25, this anomaly could indicate mined areas (voids) connecting the north entrance to the known extent of the mine. The resistivity values, however, are not in the typically expected ranges for empty (filled with air) voids. It is important to note that voids developed in gypsum and marl seams sometimes show lower resistivities compared to the resistivities observed in the voids developed inside other rock types. An example of such a condition is reported by Martínez-Moreno et al. (2015). They investigated a series of known caves developed in a gypsum/marl seam using ERT surveys. They successfully located the caves and determined the size of the caves using the ERT models but explained that the resistivities of the caves were in the range of 500–1500 ohm-m. This means that the shallow resistivity anomaly (>720 ohm-m) observed in this profile could also indicate mined areas. The low resistivities observed in the study conducted by Martínez-Moreno et al. (2015) could have been caused by the fact that the low resistivity (50 to 100 ohm-m) marl layer, where the caves were developed, was sandwiched between two gypsum layers with resistivities greater than 1000 ohm-m. The very low resistivity of the marl layer surrounding the cave could have caused the lower resistivity readings for the caves. Another, more plausible, explanation for the shallow high resistivity anomaly observed in line 1 is that it is the mined areas that are backfilled. The backfill material is probably course-grained with high permeability contrast with the surrounding layers which allows the downward seepage of the surface water (hence the negative SP values). It also reduces the resistivity of the voids as compared to air-filled voids.

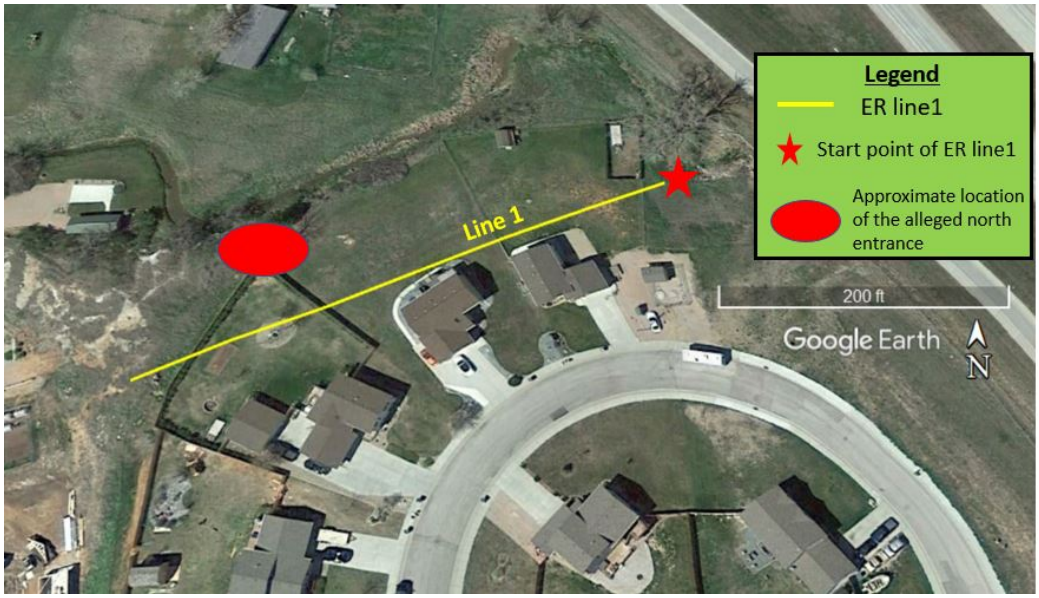

Figure 25. Location of the alleged north entrance of the mine with respect to ER line 1

Line 2 was placed on the northeast boundary of the study area (Figure 8). The ERT results indicate four distinct areas, i.e., form 50m to 65m marks, from 72.5 to 87.5 m marks, from 97.5 m to 117.5 m, and from 122.5 m to 162.5 m marks all at depths from 7.5-10 m to 15-17.5 m, with very low resistivities. According to our calculations, assuming a 10.5 degrees slope of the mine floor, these areas are at about the depth of mining if the mine had extended to this area. Also from the depth to groundwater table contour map shown in Figure 5, the depth to groundwater in this area should be around 12 to 18 m. This indicates that these four areas could in fact be the mine's working areas (voids) that are currently filled with saline water. These four tunnel-shaped areas are coincident with the negative SP data as shown in Figure 26.

Similar features are also seen along line 3, mostly with depths around 5 m to 10 m. These features, however, get deeper towards the end of the profile on the Northside which is in agreement with the general trend of mining in the area (the mine dips towards the north-northeast). Again these areas could be mined areas that were filled with saline water at the time of the investigation.

The results of ERT for lines 2 and 3 along with the known extent of the mine and the SP results are shown in Figure 26. It can be seen from this figure that areas that appear to be mined areas in line 2 coincide very well with the areas of negative SP values that indicate downward flow. This shows that the detected areas are very likely to be the mine working areas. The same agreement between the SP results and the ERT results can be seen for the portions of line 3 that overlap the SP survey area.

Line 5 has a distinct area of high resistivity in the range of expected resistivities for gypsum in the area (from 40 m to 53 m marks at a depth of 2 m to 8 m). The shallow very high resistivity part of this anomaly (>720 ohm.m) matches the high resistivity anomaly in line 1 (from 61 m to 69 m marks). They approximately have the same dimensions, orientation, and depth, which support the idea that this anomaly is an extension of the anomaly in line 1 and represents the mined areas (voids) connecting the north entrance to the known extent of the mine, and the high resistivity (but not as high as air-filled voids) could be the resistivity of backfill material. The connection between these two anomalies (the two anomalies seen in line 1 and line 5) is more clear in the fence diagram shown in Figure 27. There is also a low resistivity area from 13 m to 16 m marks at a depth of 4 m to 10 m. This area is followed by a contentious area of low resistivity that becomes shallower toward the west. The shallow part could be a conductive soil layer, a fine-grained fill area, or a disintegrating (dissolving) gypsum layer while the deeper portion at the bottom could be a mined area. More information is required to better interpret this feature, but unfortunately, this line did not extend enough to the East.

Lines 6 and 8 extend over the known mined areas. The known mined area is located between about 40 m to 50 m marks in line 6. This area was dry in 2020 when the cavers entered the mine and mapped the working areas. In the ERT model, there is a very low resistivity area in this location at a depth of 6 m to 8 m surrounded by a larger area of low resistivity. Another area of very low resistivity from 52 m to 55 m marks is also detected by the ERT model which is at a depth of 2.5 to 5 m. From the 15 m mark to the 35 m mark on this line, a large area of low resistivity is observed that is consistent with the resistivities seen on line 3 as they intersect in this location. Line 8, at about the 90 m mark, intersects with line 3 at about 180 m mark. According to both ERT models of lin 3 and line 8, there is a low resistivity area at this point at about 5 m to 10 m depths. Again, the results are consistent, and as explained before this area is likely to be a flooded mined area.

Line 7 is oriented in a north-south direction to the west of the known extent of the mine to determine the possibility of the mine extending to the west.

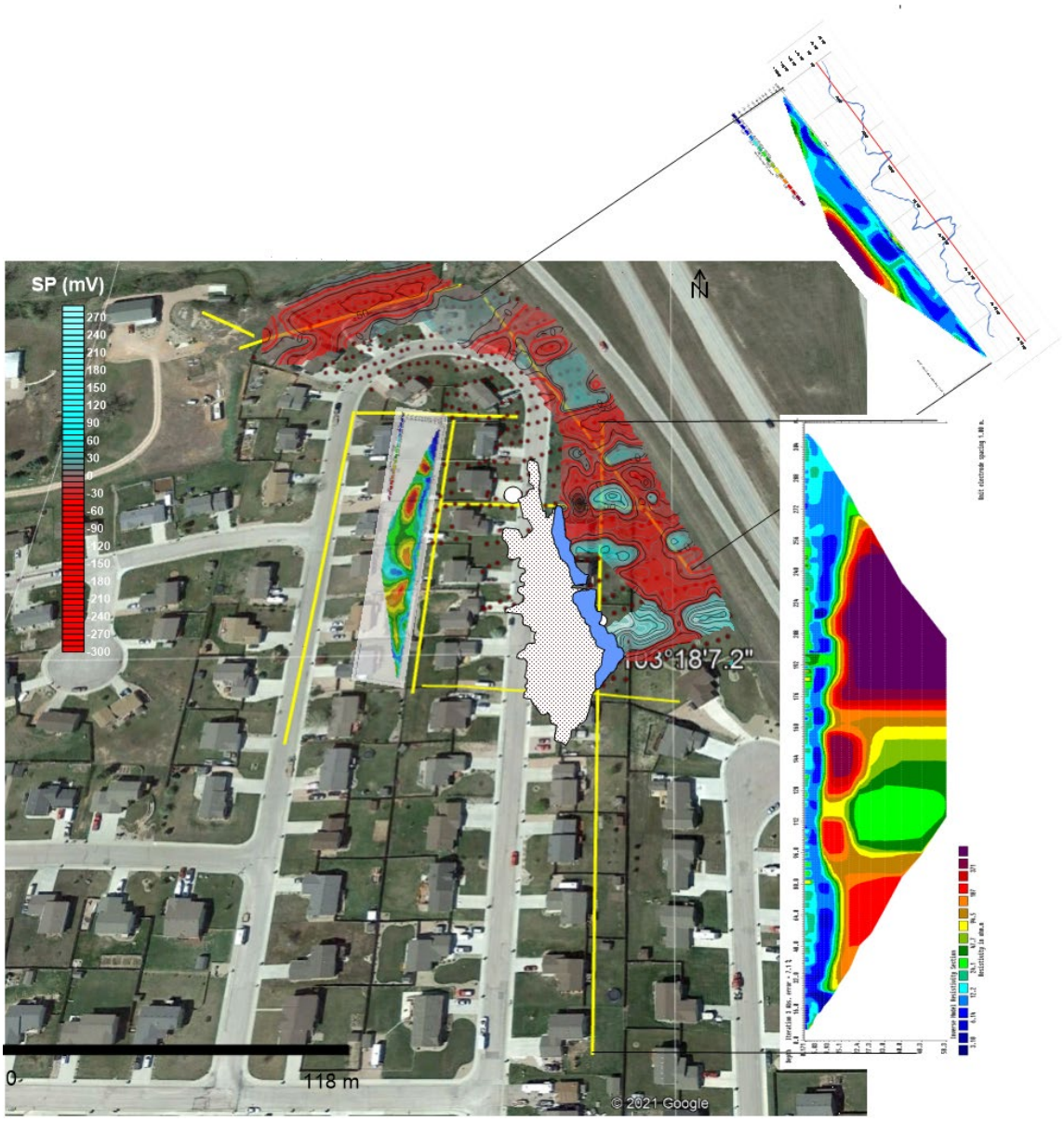

Figure 26. Comparing the SP results with the ERT results for lines 2, 3 and 7

The ERT model of line 7 shows four distinct areas with high resistivities indicated by brown to red colors. The resistivities of these areas are higher than the surrounding layers but on the lower end of the resistivity ranges seen for the gypsum in the study area. These four areas, therefore, could be either gypsum layers, collapsed areas of the mine, or mined areas that have already been backfilled. It is worth mentioning that these areas are very close to the western entries identified by some of the local residents and old areal maps dated back to 1938. It is worth noting that the area between 95 m and 97 m marks is characterized by low resistivity values squeezed between two high resistivity zones that represent a strong soil heterogeneity. The same feature is also observed at the 32 m mark. Ground depressions (settlement) corresponding to these areas were also observed on the ground surface when conducting the ER measurements. These features

could be related to deteriorating conditions (dissolution) and future potential collapses (sinkholes) could be expected in these areas.

Line 9 was the last ERT line that was conducted on the west boundary of the area. The ERT model of this line shows three areas with relatively low resistivities that extend to the surface. These could be the engineering fill that was used in the subdivision. No indication of voids or any other significant features were observed on this profile.

The ERT models developed for all the lines (except for the ERT line 4 that was conducted on the gypsum outcrop) are combined in a fence diagram as shown in Figure 27. As it can be seen in this figure, the ERT models for all lines are in very good agreement showing a big picture of the area. This figure indicates that it is very likely that the mine extends to the northeast, east, and southeast of the mapped area. It also confirms that, as was expected, the mine is dipping towards the northeast-east side and the mined areas in this direction are flooded.

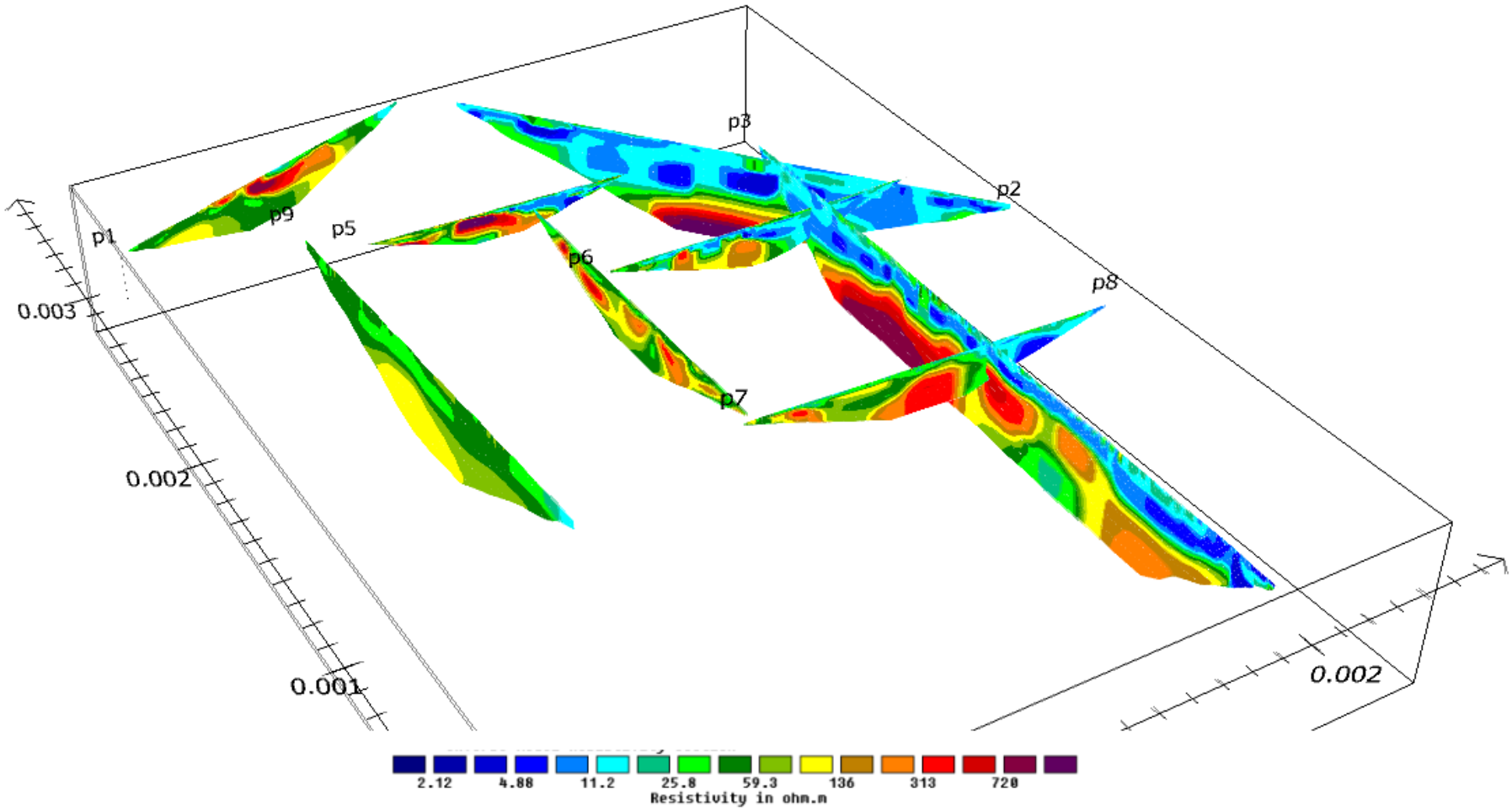

Figure 27. Fence diagram combining the ERT models of all the lines

CONCLUSIONS

Three non-destructive geophysical methods, i.e., FDEM, SP, and ERT methods, were conducted in some portions of the Hideaway Hills Subdivision, Blackhawk, SD. to identify potential voids beyond the known extent of the abandoned gypsum mine. The results of the three methods were in good agreement and helped identify several locations beyond the known extent of the mine where there is a high possibility of the existence of voids. The results show that it is very likely that the mine extends well beyond the known (mapped) areas on the northeast, east, and southeast side. Based on the information obtained in this research, there is also the possibility that the mine extends below the interstate. According to the results of this investigation, it is unlikely that the mine extends much farther to the west beyond the limits of the ERT-line 7. This conclusion is consistent with the information obtained from the residents and old areal maps that place the western entries of the mine a few feet west of the ERT-line 7. This is also in agreement with the ERT model of line 9 (conducted on the west boundary of the investigation area) where no indication of voids or any other significant features were observed.

Finally, we suggest conducting a more detailed (3-D) resistivity study on the northeast and east side of the area along with the Very Low-Frequency Electromagnetic (VLF) Method to be able to develop a detailed 3D model (map) of the mined areas in this part.

REFERENCES

Aberdeen SD. Annual report of the state mine inspector of the state of South Dakota. 1928.

Guinea A, Playà E, Rivero L, Himi M. Electrical resistivity tomography and induced polarization techniques applied to the identification of gypsum rocks. In: Near Surface Geophysics [Internet]. EAGE Publishing BV; 2010 [cited 2021 Jun 7]. p. 249–57. Available from: https://onlinelibrary.wiley.com/doi/full/10.3997/1873-0604.2010009

King M. Abandoned Mine & Quarry Accidents Claim 20-30 Lives Per Year [Internet]. 2017 [cited 2020 Dec 10]. Available from: https://geology.com/articles/abandoned-mines.shtml

Lisenbee AL, Hargrave RG. Geologic map of the Blackhawk quadrangle, South Dakota (Map Scale: 1:24,000) [Internet]. 2005. Available from: https://ngmdb.usgs.gov/Prodesc/proddesc_96362.htm

Loke MH. Rapid 2D Resisitivty & IP Inversion using the least-squares method: in Geotomo Software Manual. 1996.

Loke MH. Tutorial: 2-D and 3-D Electrical Imaging Surveys. Geotomo Software, Res2dinv 3.5 Software. 2004.

Martínez-Moreno FJ, Galindo-Zaldívar J, Pedrera A, González-Castillo L, Ruano P, Calaforra JM, et al. Detecting gypsum caves with microgravity and ERT under soil water content variations (Sorbas, SE Spain). Eng Geol. 2015 Jul 2;193:38–48.

Martínez-Moreno FJ, Santos FAM, Galindo-Zaldívar J, González-Castillo L, Pedrera A, Bernando I, et al. Characterization of a cave by means of microgravity and electrical resistivity 3D-inversions: Zé de Braga cave (Mira de Aire, Portugal). First Break [Internet]. 2018 Oct 1 [cited 2021 May 28];36(10):19–34. Available from: https://www.earthdoc.org/content/journals/10.3997/1365-2397.2018004

Minsley BJ, Burton BL, Ikard S, Powers MH. Hydrogeophysical investigations at hidden Dam, Raymond, California. J Environ Eng Geophys. 2011 Dec;16(4):145–64.

Moreno FJM. Detection and characterization of karstic caves: Integration of geological and geophysical techniques. Universidad de Granada; 2015.

NC-DEQ. Ground Collapse: Old mines and prospects and sinkholes [Internet]. [cited 2020 Dec 10]. Available from: https://deq.nc.gov/about/divisions/energy-mineral-land-resources/north-carolina-geological-survey/geologic-hazards/ground-collapse-old-mines-and-prospects-and-sinkholes

Özel S, Darıcı N. Environmental hazard analysis of a gypsum karst depression area with geophysical methods: a case study in Sivas (Turkey). Environ Earth Sci [Internet]. 2020 Mar 1 [cited 2021 Jun 2];79(5):115. Available from: https://doi.org/10.1007/s12665-020-8861-4

Revil A, Jardani A. The self-potential method: Theory and applications in environmental geosciences [Internet]. Vol. 9781107019, The Self-Potential Method: Theory and Applications in Environmental Geosciences. Cambridge University Press; 2010 [cited 2021 Jun 8]. Available from: https://www.cambridge.org/core/books/selfpotential-method/F191D8B2BBBE152F1ABA099CF648CDA3

Soupios PM, Georgakopoulos P, Papadopoulos N, Saltas V, Andreadakis A, Vallianatos F, et al. Use of engineering geophysics to investigate a site for a building foundation. J Geophys Eng [Internet]. 2007 Mar 27 [cited 2021 Jun 8];4(1):94–103. Available from: https://academic.oup.com/jge/article/4/1/94/5127677

Stafford KW, Brown WA, Ehrhart JT, Majzoub AF, Woodard JD. Evaporite karst geohazards in the delaware basin, texas: Review of traditional karst studies coupled with geophysical and remote sensing characterization. Int J Speleol [Internet]. 2017 May 7 [cited 2021 Jun 2];46(2):169–80. Available from: http://scholarcommons.usf.edu/ijs/vol46/iss2/4/

Ulugergerli EU, Akca I. Detection of cavities in gypsum. J Balk Geophys Soc. 2006;9(1):8–19.

Wolfe DA, Anderson N, Austin D, Ohms R, Pelczarski C, Springhetti D, et al. Map of Hideaway Mine-Hideaway Hills Subdivision - Sinkhole/Mine [Internet]. 2020. Available from: https://perma.cc/5D45-BWNW

Zionts A. Meade County Planning Board knew Hideaway Hills was built over mine as early as 2000 | Local | rapidcityjournal.com [Internet]. Rapid City Journal. 2020 [cited 2020 Dec 10]. Available from: https://rapidcityjournal.com/news/local/meade-county-planning-board-knew-hideaway-hills-was-built-over-mine-as-early-as-2000/article_dc405d7c-bd07-5bc6-8837-32a2216b9c07.html